Aust. J. Phys., 1996, **49**, 1121–33

Field Line Pitch and Local Magnetic Shear in Tokamaks

J. L. V. Lewandowski and M. Persson[A]

Department of Theoretical Physics and Plasma Research Laboratory,
Research School of Physical Sciences and Engineering,
Australian National University,
Canberra, ACT 0200, Australia.
Jerome.Lewandowski@anu.edu.au

[A] Present address: Institute for Electromagnetic Field Theory and
Euratom/NER Association, Chalmers University of Technology,
Göteborg, Sweden.

Abstract

The field line pitch and its relation to the integrated magnetic shear is discussed for a low-β tokamak plasma. Analytical results using a second order inverse aspect ratio expansion are presented and specifically discussed in the limits of peaked and flat current profiles. The results are compared and contrasted with an earlier calculation of the local magnetic shear.

1. Introduction

Improved tokamak performance has been obtained in configurations with significant negative global magnetic shear (Lazarus *et al.* 1991, Hugon *et al.* 1992). The global magnetic shear is a surface averaged quantity and, at least for localised modes, the local magnetic shear (Greene and Johnson 1968; Ware 1965) and the integrated shear (Dewar *et al.* 1984) are more fundamental quantities. Pressure driven modes in particular are often in the region of unfavourable curvature (Greene and Chance 1981), emphasising the importance of a local measure of the magnetic shear.

The local magnetic shear comes in as a positive definite term in the magnetohydrodynamic (MHD) energy principle (Greene and Johnson 1968) and finite local magnetic shear is hence always stabilising. However, it is important to distinguish between the local shear and the surface averaged quantity. For instance, changing the sign of the surface averaged shear can increase the magnitude of the local quantity.

In the following we will discuss the local field line pitch in tokamak plasmas. This will be compared and contrasted with an earlier calculation of the local magnetic shear. The rest of the paper is organised as follows. In the next section a brief review is presented of the equilibrium problem for low-β (the ratio of kinetic pressure to magnetic field pressure) tokamak plasmas. The Grad–Shafranov equation is solved and an analytical expression is given in this

0004-9506/96/061121$05.00

asymptotic limit. In Section 3, the integrated magnetic shear and its relation to the field line pitch is discussed. These results are then compared and contrasted with earlier calculations (Lewandowski and Persson 1995) for the local magnetic shear. The results are visualised for a few specific profiles.

2. The Equilibrium

For a toroidally symmetric equilibrium, the toroidal angle ϕ is an ignorable coordinate. The contravariant form of the magnetic field can then be written in the form (White 1989):

$$\mathbf{B} = g(\psi)\nabla\zeta + I_T(\psi)\nabla\theta_* + \delta(\psi,\theta_*)\nabla\psi \,, \tag{1}$$

where ψ is the magnetic poloidal flux, θ_* is a general poloidal angle and the general toroidal angle

$$\zeta = \phi - \lambda_*(\psi,\theta_*) \tag{2}$$

is defined in such a way (by choosing λ_*) that the magnetic field lines are straight in the (ζ,θ_*) plane. In equation (1) $2\pi g(\psi)$ is the poloidal current flowing outside the flux surface and $2\pi I_T(\psi)$ is the toroidal current flowing inside the flux surface. The last term in (1) represents the degree of nonorthogonality in the coordinate system (White 1989). In the low-β limit considered in this paper, this term vanishes.

Tokamak equilibria are governed by the Grad–Shafranov equation (Shafranov 1958; Lust and Schluter 1957; Grad and Rubin 1959):

$$\nabla\cdot\frac{\nabla\psi}{X^2 q} + q\frac{dp}{d\psi} + \frac{gq}{X^2}\frac{dg}{d\psi} = 0\,. \tag{3}$$

Here $q(\psi)$ is the safety factor and X is the distance from the axis of revolution to a point on a magnetic surface. In order to find an equilibrium, equation (3) is generally solved numerically . However, in the low-β limit considered in this paper analytical solutions can be found (Shafranov 1963, 1965; Ware and Haas 1966; Greene *et al.* 1971) order by order by expanding in the inverse aspect ratio $\epsilon \equiv a/R$, where a and R are the minor and minor radii of the plasma respectively.

To second order in such an expansion and assuming that $\beta = O(\epsilon^2)$, the flux surfaces are circles shifted to the low field side to balance the kinetic pressure. This is the well-known Shafranov (1963) shift and it can be determined from the radial part of equation (3) using standard cylindrical coordinates:

$$\Delta(r) = \frac{1}{R_0}\int_0^r \left[\frac{q^2}{r'^3}\int_0^{r'} \frac{r''^3}{q^2}\left(1 - 2\frac{{R_0}^2 q^2}{{B_0}^2 r''}\frac{dp}{dr''}\right)dr''\right]dr'\,. \tag{4}$$

The poloidal part of equation (3) similarly provides an expression for λ_* in (2):

$$\frac{\partial \lambda_*}{\partial \theta} = \frac{q\eta}{X}\left(1 - \frac{X}{\eta}\right), \tag{5}$$

where $\eta \equiv R_0[1 - \dot{\Delta}\cos(\theta)]$.

By writing the magnetic field in Clebsch form,

$$\mathbf{B} = \nabla\alpha \times \nabla\psi\,, \tag{6}$$

where $\alpha \equiv \zeta - q(\psi)\theta_*$ is the field line label, we obtain the components of the magnetic field (Shafranov 1963, 1965; Ware and Haas 1966; Greene *et al.* 1971):

$$B_\theta = \frac{B_0 r}{qR_0}\left(1 - \frac{r}{R_0}\cos\theta + \dot{\Delta}\cos\theta\right), \tag{7}$$

$$B_\phi = B_0\left(1 - \frac{r}{R_0}\cos\theta + \frac{\Delta(r)}{R_0}\right), \tag{8}$$

where terms of order ϵ^3 and higher have been neglected. The second term on the right hand side of equation (7) is due to toroidal bending and the third term is due to flux surfaces compression.

3. Integrated Local Shear

High-n ballooning modes, at marginal stability, are described by the following equation (Coppi 1977):

$$\mathbf{B}\cdot\nabla\left(\frac{|\nabla\alpha_*|^2}{B}\,\mathbf{B}\cdot\nabla\hat{\Phi}\right) + \frac{2}{|\nabla\psi|}\,\frac{dp}{d\psi}\left(\kappa_N + \kappa_G\frac{I|\nabla\psi|^2}{B^2}\right)\hat{\Phi} = 0\,, \tag{9}$$

where $\hat{\Phi}$ is the ballooning eigenfunction. Equation (9) has to be solved along the field line with appropriate boundary conditions at $\theta_* = \pm\infty$, on a given magnetic surface. Here κ_N and κ_G are the normal and geodesic curvatures respectively. The normal vector is perpendicular to the magnetic field line direction and is locally normal to a given magnetic surface. The geodesic curvature is the component of the magnetic field curvature which is perpendicular both to the normal vector and to the magnetic field direction. The integrated local shear is defined as follows:

$$I \equiv -\frac{\nabla\alpha_*\cdot\nabla\psi}{\nabla\psi\cdot\nabla\psi}\,. \tag{10}$$

Here

$$\alpha_* = \phi - \lambda_*(\psi,\theta) - q(\psi)\theta \tag{11}$$

is the field line label for a second order equilibrium. The so-called stream function λ_* is chosen so that the magnetic field lines appear to be straight; its expression can be found by direct integration of equation (5):

$$\lambda_*(\psi,\theta) = \int_{\theta_0}^{\theta} Q(\psi,\theta')d\theta' \; - \; q(\psi)(\theta-\theta_0)\,, \tag{12}$$

where it has been assumed that $\lambda_*(\psi,\theta_0)=0$. The latter is an arbitrary function of ψ (White 1989), reflecting the fact that the field lines are constrained to magnetic surfaces. Here $Q \equiv q\eta/X$ is the local pitch of the magnetic field lines, while θ_0 is the poloidal angle at which the along-the-field-line integration is started. For a second order equilibrium, the local pitch is given by

$$Q(r,\theta) = q(r)\left\{1 - \frac{r}{R_0}\left[1+\frac{\dot{\Delta}}{r}\cos(\theta)\right] + \frac{r^2}{{R_0}^2}\left[1+\frac{\dot{\Delta}}{r}\cos^2(\theta)+\frac{R_0\Delta}{r^2}\right]\right\}, \tag{13}$$

where terms of order ϵ^3 have been neglected. Using equations (11) and equation (13), we obtain an expansion for the integrated local shear, accurate to $O(1)$:

$$I = I^{(-2)} + I^{(-1)} + I^{(0)}\,, \tag{14}$$

where

$$I^{(-2)} = {R_0}^2\frac{q^2}{r^2}\hat{s}(\theta-\theta_0)\,, \tag{15}$$

$$I^{(-1)} = -R_0\frac{q^2}{r}\left\{[\sin(\theta)-\sin(\theta_0)]\left[1+R_0\ddot{\Delta}+\hat{s}\left(1+\frac{\dot{\Delta}}{r}\right)\right]+\sin(\theta)\frac{\dot{\Delta}}{r}\right\}, \tag{16}$$

$$\begin{aligned} I^{(0)} = q^2 &\left\{\hat{s}\frac{R_0\Delta}{r^2} + \frac{\dot{\Delta}}{r} + \tfrac{1}{2}\left[(\hat{s}+1)\left(1+\frac{\dot{\Delta}}{r}\right)+R_0\ddot{\Delta}+1\right]\right. \\ &\times\left.\left[\theta-\theta_0+\frac{\sin(2\theta)}{2} - \frac{\sin(2\theta_0)}{2}\right]+\sin(2\theta)\frac{\dot{\Delta}}{r}\right\}. \end{aligned} \tag{17}$$

As can be seen in the last term of equation (9), the destabilising influence of the normal curvature could be reduced when the integrated I is sufficiently large and positive. However, up to second order in ϵ, the geodesic curvature varies as $\sin(\theta)$, so that the normal curvature dominates in the last term of equation (9) near the plasma outboard ($\theta \simeq 0$). Note that a vanishing θ_0 maximises the driving force appearing in the last term of equation (9). For $\theta_0 \neq 0$, the vanishing of the integrated local shear occurs in a region where the normal curvature destabilising influence is decreased while, at the same time, the stabilising influence of the geodesic curvature is increased.

The radial variation of the pitch of the magnetic field lines provides a measure of the shear and it is natural to introduce

$$S_* \equiv \frac{r}{Q}\frac{\partial Q}{\partial r}\,. \tag{18}$$

We then note that to lowest order

$$I = \int S_* dr\,. \tag{19}$$

Expanding in powers of ϵ we get

$$S_*^{(0)} = \frac{r}{q}\frac{dq}{dr}\,, \tag{20}$$

$$S_*^{(1)} = -\frac{r}{R_0}\ \cos(\theta)\ [1 + R_0\ddot{\Delta}]\,, \tag{21}$$

$$S_*^{(2)} = \frac{r^2}{{R_0}^2}\ \left\{R_0\frac{\dot{\Delta}}{r} + \cos^2(\theta)\left[2 + R_0\frac{\dot{\Delta}}{r} + R_0\ddot{\Delta}\right]\right\}. \tag{22}$$

4. Local Magnetic Shear

The local magnetic shear (LMS) is a structural parameter of the magnetic field configuration, crucial for plasma stability. The vanishing of the local shear in bad curvature regions has been found to be associated with unstable ballooning modes (Greene and Chance 1981). In the context of ideal MHD theory, for which viscosity effects, heat flow, ohmic dissipation and resistivity are neglected, the macroscopic plasma stability could be studied by introducing small perturbations in the equilibrium configuration (Greene and Johnson 1968; Furth *et al.* 1966). Linearising in the amplitude perturbations, a variational principle could be constructed (Berstein *et al.* 1958; Greene and Johnson 1968; Furth *et al.* 1966). In the associated perturbed energy, one of the stabilising terms involves the perturbed component of the magnetic field (Greene and Johnson 1968) which, in turn, contains the local magnetic shear. Following Dewar *et al.* (1984), the LMS can be written:

$$S \equiv -\mathbf{s}\cdot(\nabla\times\mathbf{s})\,, \tag{23}$$

where

$$\mathbf{s} \equiv \frac{\mathbf{B}\times\nabla\psi}{\nabla\psi\cdot\nabla\psi} \tag{24}$$

is a vector lying in the magnetic surface along the direction of the binormal vector. The LMS vanishes when one can construct a surface that contains both the magnetic field $\mathbf{B}$ and the magnetic flux gradient vector $\nabla\psi$.

Expanding the LMS in powers of ϵ yields (Lewandowski and Persson 1995)

$$S = S^{(0)} + S^{(1)} + S^{(2)} \;, \tag{25}$$

where

$$S^{(0)} = \frac{\hat{s}}{{R_0}^3} \;, \tag{26}$$

$$S^{(1)} = -\frac{r}{{R_0}^4} \cos(\theta) \left[1 + R_0 \ddot{\Delta} + \frac{R_0 \dot{\Delta}}{r} (1 - 2\hat{s}) \right] , \tag{27}$$

$$S^{(2)} = -\frac{r}{{R_0}^4} \cos^2(\theta) \left[2\dot{\Delta} - \frac{r}{R_0} + R_0 \ddot{\Delta} \left(3\dot{\Delta} - \frac{r}{R_0} \right) + R_0 \hat{s} \frac{\dot{\Delta}^2}{r} \right.$$
$$\left. - \dot{\Delta}^2 \left[1 + \cos(\theta)^2 \left(1 - \frac{r}{R_0 \dot{\Delta}} \right) \right] \right. . \tag{28}$$

Note that the LMS scales like ${R_0}^{-3}$ as can be seen from the definition equation (23). Here $\hat{s} = (r dq/dr)/q$ is the lowest order global shear, the first term in equation (27) is the toroidal bending term, and the second and third terms are due to the Shafranov shift. These are residual contributions that average to zero on the magnetic surface. The second order term might give a positive or negative contribution to the global shear depending on the details of the equilibria.

The high-n ballooning equation can be obtained from the energy principle. The formulation begins by assuming incompressible perturbations; an eikonal ansatz for the fluid displacement is assumed, $\tilde{\Phi} = \hat{\Phi} \exp(iS)$, where the amplitude $\hat{\Phi}$ and the eikonal S are slowly varying functions of the position. For perturbations with long parallel wavelength and short perpendicular wavelength, the amplitude $\hat{\Phi}$ could be expanded in powers of the 'mode fluteness' $\tau \equiv k_{||}/k_{\perp}$. Constraints on $\hat{\Phi}^{(0)}$ and $\hat{\Phi}^{(1)}$ (where the subscripts indicate the corresponding order in τ) are obtained by minimising the parallel component of the perturbed magnetic field. A variational principle for high-n ballooning is then obtained (see for instance Freidberg 1987). Minimising the Euler–Lagrange equation for the general ballooning mode energy principle yields the high-n ballooning equation (9). Therefore, the integrated local shear equation (10) is the fraction of the LMS that survives for modes strongly elongated along the field line. Specifically, the high-n ballooning mode equation is used to determine the threshold $\beta \equiv \beta_*$ that the plasma can sustain before becoming unstable. The threshold β_* can be found by considering the limit of infinitely elongated modes, that is $\tau \longrightarrow 0$. The stabilising contribution of the perturbed magnetic field enters the high-n ballooning equation as a quantity proportional to the integrated local shear. However, for $\beta < \beta_*$, one has to consider modes with small but finite τ. The stabilising effect of the perturbed magnetic field is now described by the local magnetic shear.

As can be seen from (10) and (18), the integrated shear is a nondimensional quantity. The LMS, however, scales like ${R_0}^{-3}$. For a given equilibrium, the two quantities can be compared since R_0 is fixed.

To lowest order in ϵ, the LMS and the integrated shear do not differ and are equal to the global shear, $\hat{s} = (rdq/dr/)q$. To first order in ϵ, an extra contribution (proportional to the global shear) enters the LMS. For a specific value of the global shear (i.e. when $\hat{s} = \frac{1}{2}$), the LMS and the integrated shear are equal up to $\mathcal{O}(\epsilon)$. Since our expansion parameter ϵ does not put any restriction on the safety factor, one could compare the LMS and its integrated version for a vanishing global shear ($\hat{s} \simeq 0$). In the reversed-q profile, the position where $\hat{s} = 0$ is usually located close to the plasma edge. In this region, because of the strong pressure gradient, one has $\ddot{\Delta} \ll \dot{\Delta}$ so that the integrated shear is approximatively given by $S_* \sim -r/R_0 \cos(\theta)$ which has the same poloidal dependence at the normal curvature, a destabilising contribution. In this low-shear regime, the second order contributions also become important and from equation (28) and (22), it is clear that the LMS and the integrated shear are quite different.

For the following specific cases we use the plasma pressure

$$p(r) = p(0)[1 - (r/a)^2]\,, \tag{29}$$

and, except for the case with negative shear, the q profile

$$q(r) = q(0)(1 + (r/a)^{2\lambda}[(q(a)/q(0))^{\lambda} - 1])^{1/\lambda} \tag{30}$$

as free functions. The safety factor profile for the negative global shear regime is given by a polynomial of the form:

$$q(r) = q(0)[1 + \xi_1 r/a \ + \xi_2 (r/a)^2]\,, \tag{31}$$

where ξ_1 and ξ_2 are chosen so that $dq/dr = 0$ at $r/a = 0{\cdot}5$ and so that the safety factor at the plasma edge $[q(a)]$ is the same as the one given in equation (30).

In Fig. 1 the Shafranov coordinates for a low-β tokamak are displayed. The inverse aspect ratio for this case is $\epsilon = 0.\ 3$ and the central $\beta = 4\%$. Note the Shafranov shift ($\Delta/R_0 \sim \epsilon^2$) of the circular magnetic surfaces. For a peaked q profile, $\lambda = 1{\cdot}2$ (see Fig. 2a), the region of negative integrated shear is nearly circular and slightly shifted to the plasma outboard (because of the influence of the Shafranov shift). The lowest order in the expansion for the integrated local shear is proportional to the global shear.

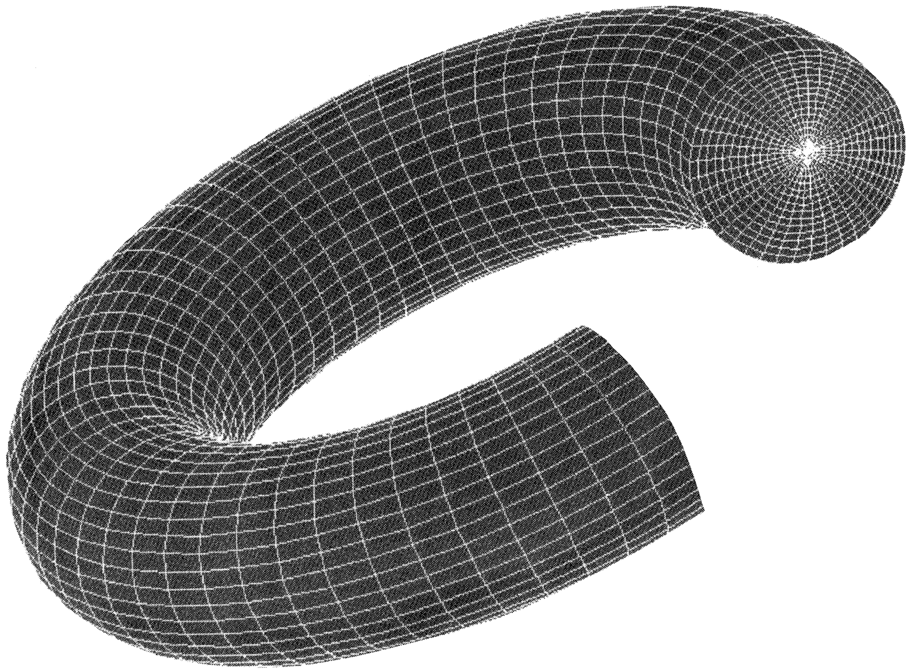

Fig. 1. Shafranov coordinates for a tokamak with central $\beta = 4 \cdot 0\%$ and inverse aspect ratio $\epsilon = 0 \cdot 3$.

For a flat q profile, $\lambda = 4 \cdot 0$ (see Fig. 3a), the global shear is small and the poloidal dependence of the integrated shear, the first order term in the expansion, plays an important role. The region of negative integrated shear is increased. When the aspect ratio is large ($\epsilon = 0 \cdot 1$) (see Fig. 4a) the toroidicity effects are small. The region of negative integrated shear is substantial but not as extended as in Fig. 3a.

Finally, in the negative global shear regime (Fig. 5a), the integrated shear is strongly negative since its lowest order contribution is negative. Note that the bean-type shape of the negative $\mathcal{S}_\star$ region extends close to the outside of the torus, where the normal curvature has a strongly destabilising influence.

For the sake of comparison, the local magnetic shear has been displayed (see Figs 2b, 3b, 4b and 5b) for the same parameters used to calculate the integrated shear. In Fig. 2b, the plasma centre is characterised by a negative LMS; in this region, the global magnetic shear is negligible so that the first order contribution in equation (25) dominates. In Fig. 3b, the aspect ratio is small but the current profile is centrally peaked. The (positive) global shear is strong but the small aspect ratio tends to increase the region of negative LMS. For a small aspect ratio and a flat current profile, the global shear is rather small and the region of negative LMS is now extended towards the plasma outboard, as shown in Fig. 4b. Finally, in the negative global shear regime (Fig. 5b), the region of negative LMS extends in the whole region of bad curvature.

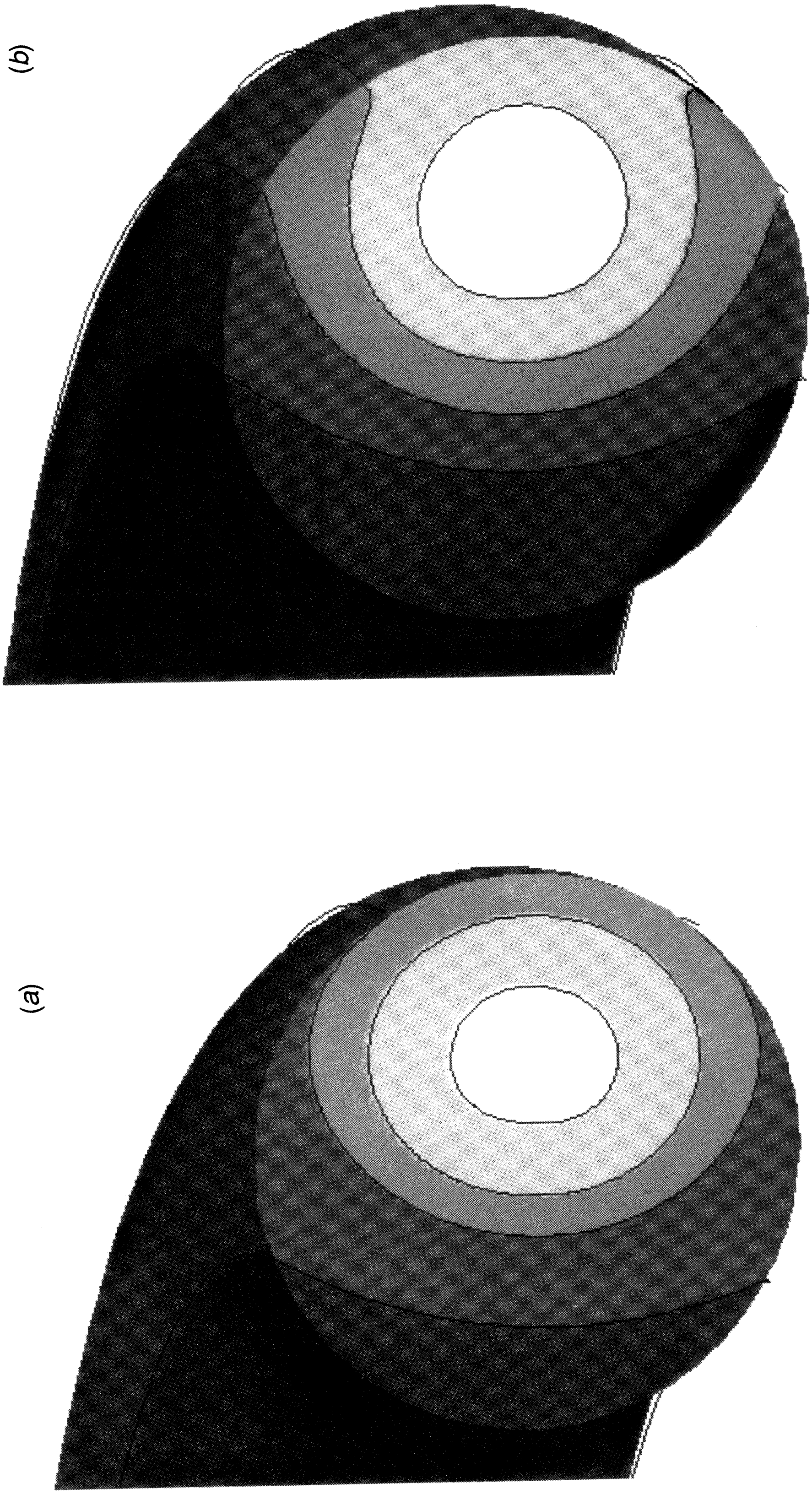

Fig. 2. (*a*) The integrated shear for a second order equilibrium, with central $\beta = 2{\cdot}0\%$, $q(0) = 1{\cdot}1$, $q(a) = 2{\cdot}4$, $\epsilon = 0{\cdot}3$ and $\lambda = 1{\cdot}2$. (*b*) The local magnetic shear (LMS) for a second order equilibrium, with central $\beta = 2{\cdot}0\%$, $q(0) = 1{\cdot}1$, $q(a) = 2{\cdot}4$, $\epsilon = 0{\cdot}3$ and $\lambda = 1{\cdot}2$. In both parts positive values of the shear are shown in grey scaling with equal intervals, while negative values are shown in white.

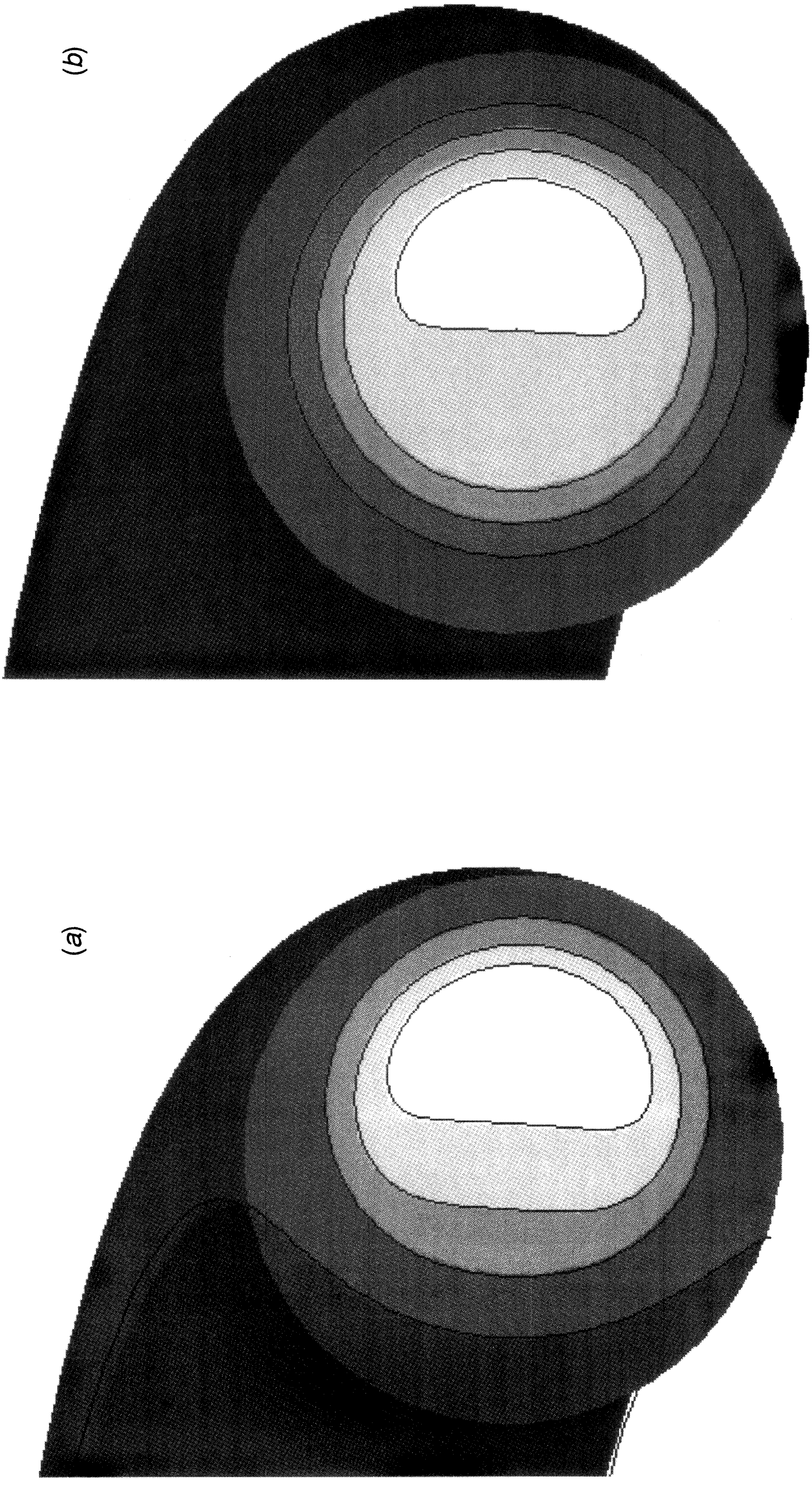

Fig. 3. Same as Fig. 2 except that $\lambda = 4 \cdot 0$.

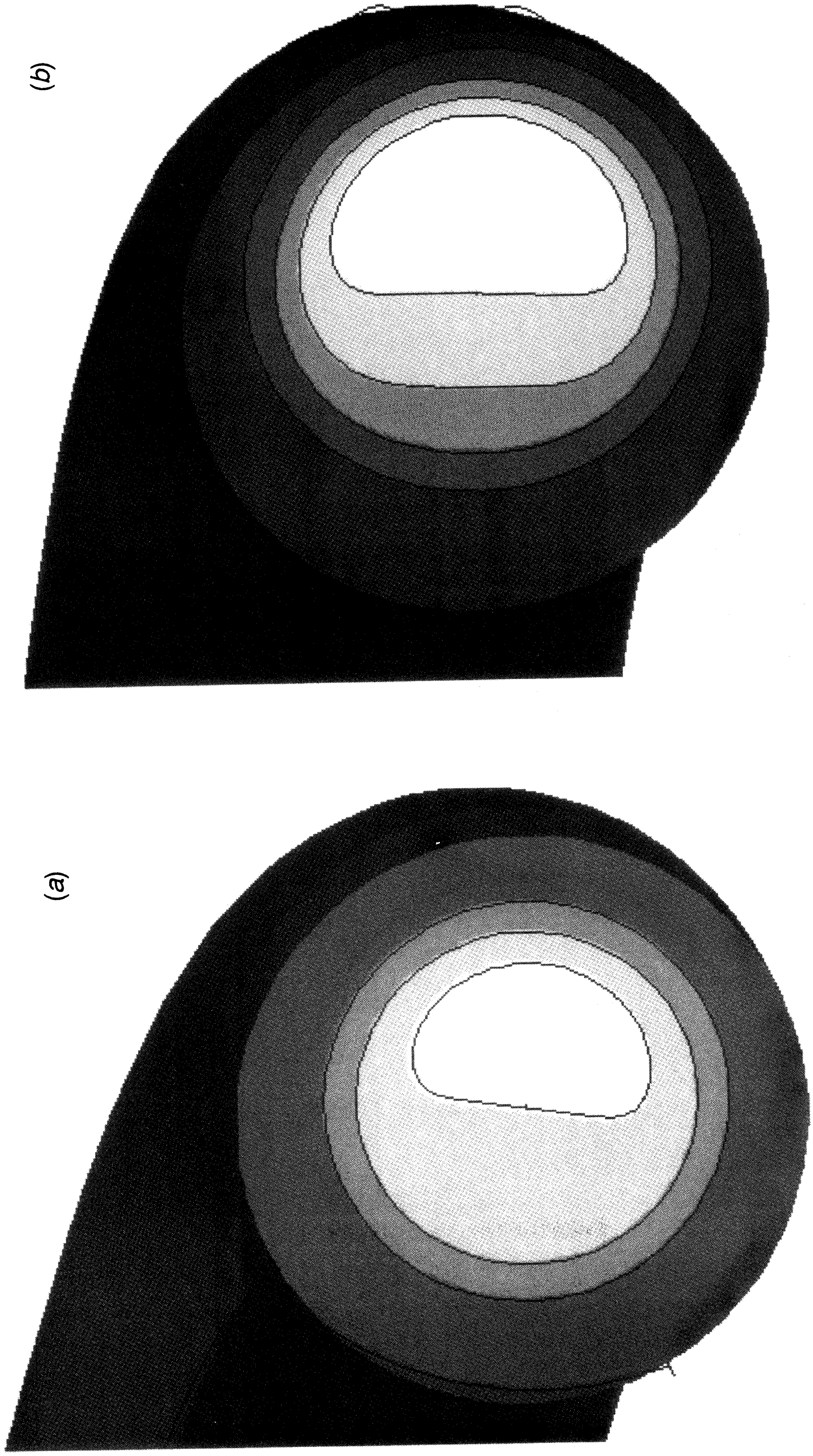

Fig. 4. Same as Fig. 2 except that $\lambda = 4 \cdot 0$, $\epsilon = 0 \cdot 1$ and $\beta = 0 \cdot 5\%$.

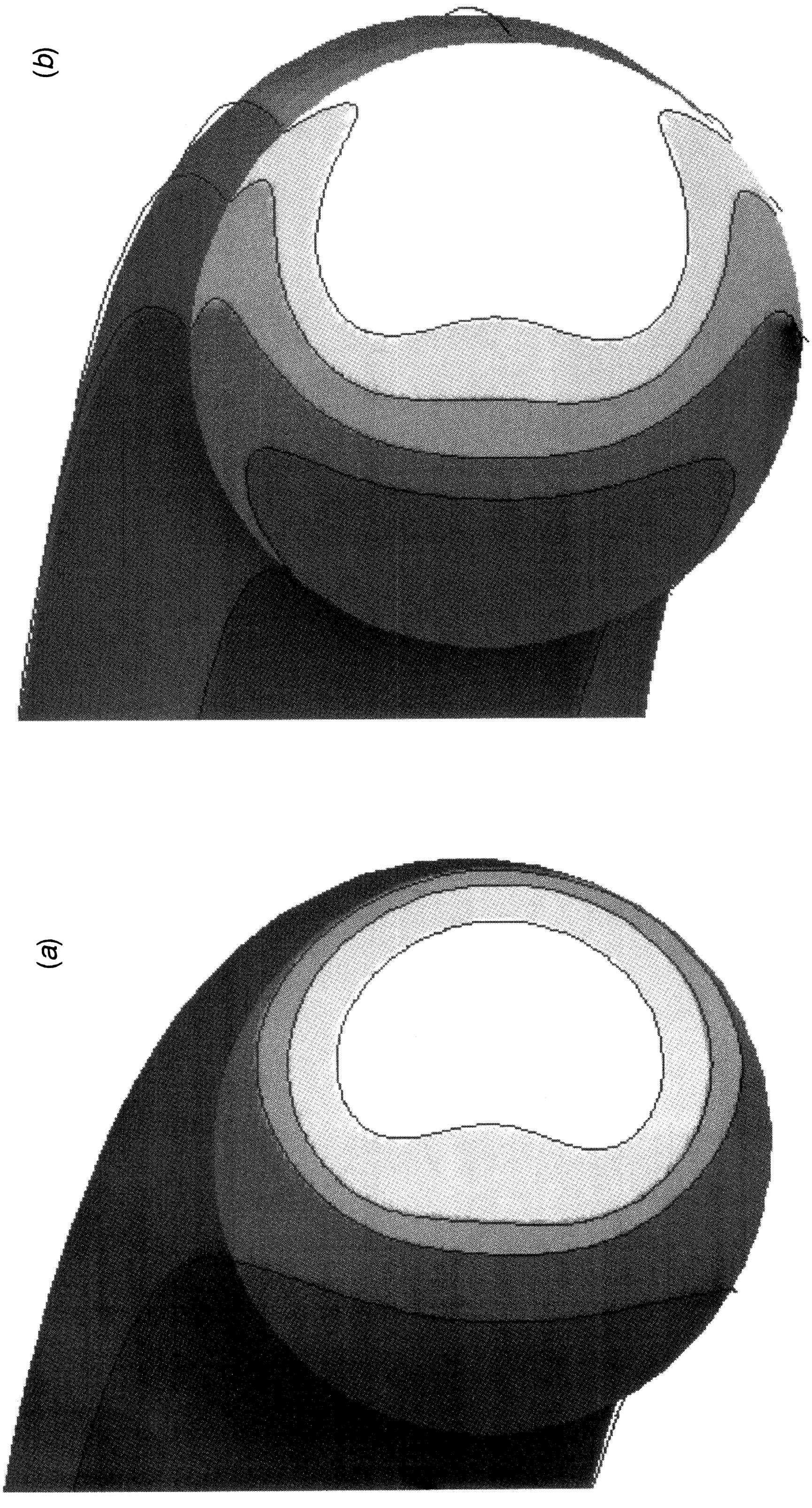

Fig. 5. Same as Fig. 2 but with negative global shear for $r < 0{\cdot}5a$.

References

Berstein, I. B., Frieman, E. A., Kruskal, M. D., and Kulsrud, R. M. (1958). *Proc. R. Soc. London* A **244**, 17.

Connor, W., Hastie, R. J., and Taylor, J. B. (1978). *Phys. Rev. Lett.* **40**, 396.

Coppi, B. (1977). *Phys. Rev. Lett.* **39**, 939.

Dewar, R. L., Monticello, D. A., and Sy, W. N.-C. (1984). *Phys. Fluids* **27**, 1723.

D'Haeseler, W. D., Hitchon, W. N. G., Callen, J. D., and Shohet, A. H. (1991). 'Flux Coordinates and Magnetic Field Structure' (Springer: Heidelberg).

Freidberg, J. P. (1987). *In* 'Ideal Magnetohydrodynamics' (Plenum: New York).

Furth, H. P., Killeen, J., Rosenbluth, M. N., and Coppi, B. (1966). 'Plasma Physics and Controlled Fusion Research', Vol. 1, p. 617 (IAEA: Vienna).

Gerver, M. J., Kesner, J., and Ramos, J. J. (1988). *Phys. Fluids* **31**, 2674.

Grad, H., and Rubin, H. (1959). Proc. 2nd United Nations Int. Conf. on the Peaceful Uses of Atomic Energy, Geneva, Vol. 31, p. 190 (Columbia University Press: New York).

Greene, J. M. (1983). *Commun. Pure Appl. Math.* **36**, 537.

Greene, J. M., and Chance, M. S. (1981). *Nucl. Fusion* **21**, 453.

Greene, J. M., and Johnson, J. L. (1968). *Plasma Phys.* **10**, 729.

Greene, J. M., Johnson, J. L., and Weimer, K. E. (1971). *Phys. Fluids* **14**, 671.

Hirose, A., Zhang, L., and Elia, M. (1994). *Phys. Rev. Lett.* **72**, 3993.

Hugon, M., Milligen, B. P., Smeulders, P., Appel, L. C., Gowers, C. W., Jacquinot, J. J., Porte, L., Rebut, P. H., Tibone, F., Tubbing, B. J. D., Watkins, M. L., and Zwingmann, W. (1992). *Nucl. Fusion* **32**, 33.

Kessel, C., Manickam, J., Rewoldt, G., and Tang, W. M. (1994). *Phys. Rev. Lett.* **72**, 1212.

Lazarus, E. A., Chu, M. S., Ferron, J. R., Helton, F. J., Hogan, J. J., Kellman, A. G., Lao, L. L., Lister, J. B., Taylor, T. S., and Turnbull, A. D. (1991). *Phys. Fluids* B **3**, 2220.

Lewandowski, J. L. V., and Persson, M. (1995). *Plasma Phys. Cont. Fusion* **37**, 1199.

Lùst, R., and Schlúter, A. (1957). *Z. Naturforsch.* **12a**, 850.

Nordman, H., Jarmén, A., Malinov, P., and Persson, M. (1995). *Phys. Plasmas* **2**, 3440.

Shafranov, V. D. (1958). *Sov. Phys. JETP* **6**, 545.

Shafranov, V. D. (1963). *J. Nucl. Energy* **C5**, 251.

Shafranov, V. D. (1965). *In* 'Reviews of Plasma Physics' (Ed. M. A. Leontovich), Vol. 2, p. 103 (Consultants Bureau: New York).

Waltz, R. E., and Boozer, A. H. (1993). *Phys. Fluids* B **5**, 2201.

Ware, A. A. (1965). Culham Laboratory Report CLM-M53 (unpublished).

Ware, A. A., and Haas, F. A. (1966). *Phys. Fluids* **9**, 956.

White, R. B. (1989). 'Theory of Tokamak Plasmas' (North Holland: Amsterdam).

Manuscript received 27 March, accepted 30 May 1996